© 2017. Published by The Company of Biologists Ltd | Development (2017) 144, 1328-1338 doi:10.1242/dev.143719

RESEARCH ARTICLE

FGF signaling enforces cardiac chamber identity in the developing ventricle

Arjana Pradhan[1], Xin-Xin I. Zeng[1], Pragya Sidhwani[1], Sara R. Marques[2], Vanessa George[3], Kimara L. Targoff[3], Neil C. Chi[4] and Deborah Yelon[1,*]

ABSTRACT

Atrial and ventricular cardiac chambers behave as distinct subunits with unique morphological, electrophysiological and contractile properties. Despite the importance of chamber-specific features, chamber fate assignments remain relatively plastic, even after differentiation is underway. In zebrafish, Nkx transcription factors are essential for the maintenance of ventricular characteristics, but the signaling pathways that operate upstream of Nkx factors in this context are not well understood. Here, we show that FGF signaling plays an essential part in enforcing ventricular identity. Loss of FGF signaling results in a gradual accumulation of atrial cells, a corresponding loss of ventricular cells, and the appearance of ectopic atrial gene expression within the ventricle. These phenotypes reflect important roles for FGF signaling in promoting ventricular traits, both in early-differentiating cells that form the initial ventricle and in late-differentiating cells that append to its arterial pole. Moreover, we find that FGF signaling functions upstream of Nkx genes to inhibit ectopic atrial gene expression. Together, our data suggest a model in which sustained FGF signaling acts to suppress cardiomyocyte plasticity and to preserve the integrity of the ventricular chamber.

KEY WORDS: Atrium, Ventricle, Amhc, Vmhc, *Nkx2.5*, Zebrafish

INTRODUCTION

The vertebrate heart is divided into atrial and ventricular chambers that work together to drive circulation, yet have unique morphological, electrophysiological and contractile attributes (Barth et al., 2005; McGrath and de Bold, 2009). These chamber-specific characteristics reflect the distinct molecular traits of atrial and ventricular cardiomyocytes: for example, each chamber expresses particular transcription factors (Bao et al., 1999; Bruneau et al., 2001; Wu et al., 2013; Xin et al., 2007), utilizes specific myosin isoforms (Berdougo et al., 2003; Bisaha and Bader, 1991; Yelon et al., 1999; Yutzey et al., 1994) and possesses discrete ion channel components (Flagg et al., 2008). Despite the well-established differences between atria and ventricles, our understanding of the mechanisms that regulate these features remains incomplete.

Fate-mapping studies in chick and zebrafish have demonstrated that atrial and ventricular lineages are separate and spatially organized in the early embryo (Garcia-Martinez and Schoenwolf, 1993; Keegan et al., 2004; Redkar et al., 2001; Stainier et al., 1993). The early diversification of these lineages is indicated by distinct gene expression programs that are evident even before the heart tube assembles (Berdougo et al., 2003; Yelon et al., 1999; Yutzey et al., 1994). For example, in zebrafish, the expression patterns of *atrial myosin heavy chain* (*amhc*; *myh6* – Zebrafish Information Network) and *ventricular myosin heavy chain* (*vmhc*) in the anterior lateral plate mesoderm correlate with the spatial organization of atrial and ventricular precursors within this tissue (Berdougo et al., 2003; Schoenebeck et al., 2007; Yelon et al., 1999). These initial populations of atrial and ventricular cells are later joined by late-differentiating cells that contribute to the venous and arterial poles of the heart and assume atrial and ventricular identity accordingly (de Pater et al., 2009; Hami et al., 2011; Kelly, 2012; Lazic and Scott, 2011; Zhou et al., 2011).

The allocation of progenitor cells into atrial and ventricular lineages is subsequently reinforced by chamber-specific transcription factors that promote the maintenance of atrial and ventricular characteristics. In mice, the atrial transcription factor COUP-TFII (Nr2f2 – Mouse Genome Informatics) regulates the atrial gene expression program (Wu et al., 2013). Tissue-specific deletion of COUP-TFII in differentiated myocardium results in ventricularized atria that express ventricular markers and exhibit electrical activity similar to that of ventricular cells. Likewise, the ventricular transcription factors Irx4 and Hey2 are both required to prevent ectopic activation of atrial genes in the ventricular myocardium (Bao et al., 1999; Bruneau et al., 2001, 2000; Koibuchi and Chin, 2007; Xin et al., 2007). Thus, atrial and ventricular chamber identities are relatively plastic and require active enforcement by chamber-specific transcription factors; however, it is not yet clear how the chamber-specific expression of these factors is established.

Our recent work in zebrafish has indicated that Nkx transcription factors play important roles in controlling regionalized expression of Irx4 and Hey2 and in maintaining ventricular identity (Targoff et al., 2013). Both *irx4a* and *hey2* are downregulated in *nkx2.5*; *nkx2.7* double mutants; furthermore, loss of Nkx gene function leads to gradual reduction of *vmhc* expression and simultaneous gain of *amhc* expression within the ventricle, ultimately yielding an expanded atrium, a diminished ventricle, and ectopic *amhc*-expressing cells within the ventricular remnant. In addition, Nkx genes promote the attainment of ventricular characteristics in the late-differentiating cells that append to the arterial pole (George

[1]Division of Biological Sciences, University of California, San Diego, La Jolla, CA 92093, USA. [2]Developmental Genetics Program and Department of Cell Biology, Kimmel Center for Biology and Medicine, Skirball Institute of Biomolecular Medicine, New York University School of Medicine, New York, NY 10016, USA. [3]Division of Cardiology, Department of Pediatrics, College of Physicians and Surgeons, Columbia University, New York, NY 10032, USA. [4]Division of Cardiovascular Medicine, Department of Medicine, University of California, San Diego, La Jolla, CA 92093, USA.

*Author for correspondence (dyelon@ucsd.edu)

A.P., 0000-0002-4119-6121; X.-X.I.Z., 0000-0002-2707-7759; P.S., 0000-0002-5292-6740; S.R.M., 0000-0002-5869-2260; V.G., 0000-0003-1990-4651; K.L.T., 0000-0002-6066-6002; N.C.C., 0000-0003-2324-3796; D.Y., 0000-0003-3523-4053

Received 12 August 2016; Accepted 13 February 2017

Development (2017) 144, 1328-1338 doi:10.1242/dev.143719

et al., 2015). Thus, Nkx genes seem to sit near the top of the transcriptional hierarchy that ensures retention of ventricular identity in both early-differentiating and late-differentiating cardiomyocytes.

We now seek to define the signaling pathways that act upstream of Nkx genes to control the maintenance of ventricular identity. One appealing candidate is the FGF signaling pathway, as prior studies have demonstrated its influence on the induction of *nkx2.5* expression and on the regulation of ventricular size. In zebrafish, chick and *Xenopus*, *nkx2.5* expression in the anterior lateral plate mesoderm is significantly reduced when the FGF pathway is inhibited (Alsan and Schultheiss, 2002; Keren-Politansky et al., 2009; Reifers et al., 2000; Simões et al., 2011). Additionally, inhibiting FGF signaling during gastrulation in zebrafish reduces the number of cells in both cardiac chambers, with a stronger impact on the ventricle (Marques et al., 2008). This early influence of FGF signaling is echoed at later stages, when FGF signaling promotes the accretion of late-differentiating cells to the arterial pole of the ventricle (de Pater et al., 2009; Lazic and Scott, 2011; Marques et al., 2008; Zeng and Yelon, 2014). Similarly, in mouse, a hypomorphic allele of *Fgf8* or tissue-specific deletion of *Fgf8* results in formation of a hypoplastic right ventricle and outflow tract (Abu-Issa et al., 2002; Ilagan et al., 2006; Park et al., 2006).

Here, we demonstrate a previously unappreciated role for FGF signaling during ventricular development: in addition to promoting the allocation of an appropriate number of ventricular cardiomyocytes, FGF signaling ensures that these cells properly maintain their ventricle-specific characteristics. We find that inhibiting FGF signaling subsequent to the onset of chamber-specific differentiation leads to a gradual accumulation of atrial cells, a corresponding loss of ventricular cells, and a progressive increase in the appearance of ectopic *amhc*-expressing cells in the ventricle. Examination of the dynamic localization of Vmhc and Amhc, as well as analysis of *amhc*-expressing cells using a photoconvertible reporter transgene, suggests that sustained FGF signaling is required to repress the acquisition of atrial traits by ventricular cardiomyocytes. This role of FGF signaling influences the retention of ventricular characteristics both in the early-differentiating cells that form the initial ventricle and in the late-differentiating cells that contribute to the arterial pole. Finally, we demonstrate that FGF signaling acts upstream of Nkx genes to execute its important function in enforcing ventricular identity. Together, our studies provide insight into the mechanisms regulating plasticity and commitment of ventricular cardiomyocytes, both of which are fundamentally important for strategies in cardiac regenerative medicine.

RESULTS

Inhibition of FGF signaling results in ectopic *amhc* expression in the ventricle

Zebrafish *fgf8a* mutants have small hearts with severe deficiencies in the size of both the atrium and the ventricle (Marques et al., 2008; Reifers et al., 2000). Our prior work has shown that FGF signaling plays an early role in promoting the production of both atrial and ventricular cardiomyocytes, with a particularly potent effect on ventricular cardiomyocytes (Marques et al., 2008). This function of FGF signaling accounts for the small cardiac chambers in *fgf8a* mutants, but there remains an unexplained aspect of the *fgf8a* mutant phenotype: in contrast to wild-type hearts (Fig. 1A,E), *fgf8a* mutant hearts express *amhc* not only in the atrium, but also in a separate cluster of cardiomyocytes in the ventricle, clearly outside of the normal domain of *amhc* expression (Fig. 1B,F). (Here, we will refer to these as 'ectopic *amhc*-expressing cells'.) This scenario is reminiscent of the phenotype of *nkx2.5* mutants, which initially exhibit normal expression patterns of *amhc* and *vmhc*, but then display ectopic *amhc*-expressing cells at later stages (George et al., 2015; Targoff et al., 2013). We therefore explored whether this aspect of the *fgf8a* mutant phenotype reflected a later role for FGF signaling in preventing inappropriate *amhc* expression, in addition to its earlier influence on the initial production of ventricular cells.

To evaluate whether FGF signaling plays a relatively late role in repressing ectopic *amhc* expression, we inhibited the FGF pathway at stages after the onset of atrial and ventricular differentiation. Because expression of both *amhc* and *vmhc* is initiated by 18 h post-fertilization (hpf) (Fig. S1), we chose to reduce FGF signaling from this stage onwards. We employed two methods to manipulate FGF signaling: heat-induced expression of a dominant-negative form of Fgfr1, using the transgene *Tg(hsp70l:dnfgfr1-EGFP)* (Lee et al., 2005) [hereafter referred to as *Tg(hsp70:dnfgfr1)*], and exposure to the FGFR antagonist SU5402 (Mohammadi et al., 1997). Using either method, inhibition of FGF signaling starting at 18 hpf consistently generated ectopic *amhc*-expressing cells, most notably in the ventricular inner curvature and near the arterial pole (Fig. 1C, D,G,H). These data show that FGF signaling prevents inappropriate *amhc* expression in the ventricle; moreover, FGF signaling has a sustained influence on ventricular development, beyond its previously demonstrated role in the early embryo (Marques et al., 2008).

At 18 hpf, *fgf8a* is expressed in and near ventricular precursors, and it continues to be expressed in the ventricle through 48 hpf (Reifers et al., 2000). This persistence of *fgf8a* expression prompted us to investigate the duration over which FGF signaling is required to prevent ventricular expression of *amhc*. As seen at 18 hpf, administration of heat shock to *Tg(hsp70:dnfgfr1)* embryos at 24 or 28 hpf also generated ectopic *amhc*-expressing cells (Fig. 2), whereas ectopic *amhc*-expressing cells were not seen in embryos after heat shock at 29, 30 or 31 hpf (data not shown; $n \geq 10$ for each stage). Additionally, we observed differences in the potency of the effect of expressing *Tg(hsp70:dnfgfr1)* at 18, 24 and 28 hpf. Whereas all embryos heat shocked at 18 hpf (n=15/15) and nearly all embryos heat shocked at 24 hpf (n=22/24) displayed ectopic *amhc*-expressing cells, only a small number of embryos heat shocked at 28 hpf (n=6/36) exhibited this phenotype. Also, whereas embryos heat shocked at 18 hpf typically displayed ectopic *amhc*-expressing cells both in the inner curvature and at the arterial pole (Fig. 1C,G), fewer ectopic *amhc*-expressing cells were detected, primarily at the arterial pole, after heat shock at 24 hpf (Fig. 2B,E), and even fewer ectopic *amhc*-expressing cells were seen at the arterial pole after heat shock at 28 hpf (Fig. 2C,F). Together, these results suggest that FGF signaling is required until approximately 28 hpf to repress ectopic expression of *amhc* within the ventricle, although this requirement tapers over time.

Loss of FGF signaling results in progressive accumulation of atrial cells and simultaneous loss of ventricular cells

In addition to creating ectopic *amhc*-expressing cells in the ventricle, loss of FGF signaling at 18 hpf also alters chamber morphology, such that the atrium appears abnormally dilated and the ventricle appears abnormally compact (Fig. 1E,G,H). These aberrant morphologies seem to be the consequence of an altered number of cardiomyocytes in each chamber: for example, following heat shock at 18 hpf, *Tg(hsp70:dnfgfr1)* embryos exhibited an increased number of $Amhc^{+}$ cells and a decreased number of $Amhc^{-}$ cells at 50 hpf (Fig. 3E-G), but their total number of

Development (2017) 144, 1328-1338 doi:10.1242/dev.143719

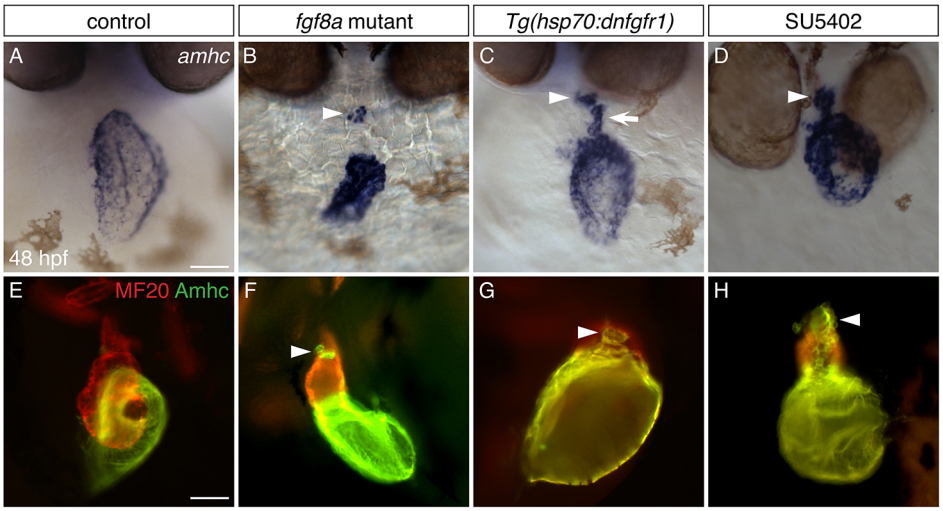

Fig. 1. Inhibition of FGF signaling results in ectopic *amhc* expression in the ventricle. (A-D) *In situ* hybridization showing *amhc* expression in frontal views at 48 hpf. (A) Wild-type embryos express *amhc* in the atrium. Similar phenotypes are seen in all controls examined: wild-type siblings of *fgf8a* mutants, nontransgenic siblings following heat shock, and DMSO-treated siblings. (B) In *fgf8a* mutants, *amhc* expression is found not only in the atrium but also in a small cluster of ventricular cells (arrowhead; *n*=32/46 mutants). (C) More ectopic *amhc*-expressing cells are induced in *Tg(hsp70:dnfgfr1)* embryos following heat shock at 18 hpf (*n*=15/15); these cells are typically seen along the inner curvature (arrow) and at the arterial pole (arrowhead) of the ventricle. (D) Similarly, ectopic *amhc*-expressing cells can be induced by exposure to SU5402 starting at 18 hpf (arrowhead; *n*=15/15). The relatively mild phenotype of *fgf8a* mutants (B), compared with the more striking presence of ectopic cells in *Tg(hsp70:dnfgfr1)*-expressing and SU5402-treated embryos (C,D), suggests that additional FGF ligands might work together with *fgf8a* to prevent inappropriate *amhc* expression. (E-H) Immunofluorescence with MF20 (marks the myocardium; red) and S46 (recognizes Amhc; green) showing cardiac morphology and Amhc localization in lateral views at 48 hpf. In contrast to wild type (E), ectopic Amhc (arrowheads) is seen in *fgf8a* mutants (F), *Tg(hsp70:dnfgfr1)* embryos after heat shock at 18 hpf (G) and embryos treated with SU5402 from 18-30 hpf (H) (*n*>10 each). Scale bars: 50 µm.

cardiomyocytes remained the same (Fig. 3G). This phenotype emerged gradually over time in *Tg(hsp70:dnfgfr1)* embryos. In the linear heart tube, only a modest increase in the number of Amhc$^+$ cells was detectable (Fig. 3A,B,G). This excess of Amhc$^+$ cells became more substantial by 36 hpf (Fig. 3C,D,G) and was most notable at 50 hpf (Fig. 3E-G). At all stages examined, we found reciprocal changes in the numbers of Amhc$^+$ and Amhc$^-$ cells, such that the total number of cardiomyocytes was not significantly altered (Fig. 3G). Moreover, the observed increase in Amhc$^+$ cells was primarily driven by changes within the atrial chamber, with ectopic Amhc$^+$ cells in the ventricle providing only a minor contribution to the total Amhc$^+$ number. At 26.5 hpf, we occasionally saw one ectopic Amhc$^+$ cell in *Tg(hsp70:dnfgfr1)* embryos, and at 36 and 50 hpf ectopic cells constituted around 10% of the total Amhc$^+$ population (Table S1). Thus, in addition to preventing ectopic *amhc* expression in the ventricle, FGF signaling also plays an important role in preserving the relative proportions of the ventricle and the atrium. Intriguingly, the gradual and reciprocal shift in chamber proportions observed in *Tg(hsp70:dnfgfr1)* embryos echoes the phenotype seen in Nkx-deficient embryos, in which cardiomyocytes appear to undergo a ventricular-to-atrial transformation (Targoff et al., 2013). This similarity suggests that FGF signaling, like Nkx genes, promotes the maintenance of chamber proportions, possibly by preventing a conversion from ventricular to atrial identity.

Loss of FGF signaling results in increased expression of *amhc* and decreased expression of *vmhc* in the ventricle

Bearing in mind the notion that a shift in chamber proportions could result from a ventricular-to-atrial fate transformation (Targoff et al., 2013), we wondered whether the appearance of ectopic *amhc*-expressing cells in embryos lacking FGF signaling might also reflect a defect in maintaining ventricular identity. Does aberrant *amhc* expression arise within resident ventricular cardiomyocytes, or do the ectopic *amhc*-expressing cells originate elsewhere and then enter the ventricle? As a first step towards understanding the origins of the ectopic *amhc*-expressing cells, we investigated the dynamics of *amhc* and *vmhc* expression following inhibition of FGF signaling. Our analysis in *Tg(hsp70:dnfgfr1)* embryos indicated that ectopic *amhc*-expressing cells emerged with a characteristic spatial organization in the ventricle (Fig. 4A-H). These cells first appeared between 26 and 29 hpf along the inner curvature of the ventricle (Fig. 4E,F) and were later observed both along the inner curvature and at the arterial pole (Fig. 4G,H). Expression of *vmhc* was compromised in a reciprocal fashion when FGF signaling was inhibited (Fig. 4I-P). Reduced *vmhc* expression became apparent between 26 and 29 hpf (Fig. 4M,N), and, at later stages, *vmhc* expression appeared to be excluded from the portions of the ventricle that contained ectopic *amhc* expression (Fig. 4O,P). Together, the dynamics of *amhc* and *vmhc* expression in *Tg(hsp70:dnfgfr1)* embryos suggest that FGF signaling not only prevents ectopic *amhc* expression in the ventricle but also preserves ventricular expression of *vmhc*.

Given that FGF signaling inhibits *amhc* expression and promotes *vmhc* expression in the ventricle, we investigated whether it is also capable of repressing *amhc* expression and inducing ectopic *vmhc* expression in the atrium. For these studies, we employed the transgene *Tg(hsp70:ca-fgfr1)*, which facilitates activation of FGF signaling through heat-inducible expression of a constitutively active form of Fgfr1 (Marques et al., 2008). Although activation of *Tg(hsp70:ca-fgfr1)* at early stages can generate a surplus of cardiomyocytes (Marques et al., 2008; Sorrell and Waxman, 2011), we found that induction of transgene expression at 18 hpf did not alter the distribution of *amhc* expression (Fig. S2A,B), nor did it introduce ectopic *vmhc* expression (Fig. S2C,D). Thus, FGF signaling is not sufficient to regulate *amhc* or *vmhc* expression in the context of the atrium; its role in controlling the expression of *amhc* and *vmhc* seems to be restricted to the ventricle.

Development (2017) 144, 1328-1338 doi:10.1242/dev.143719

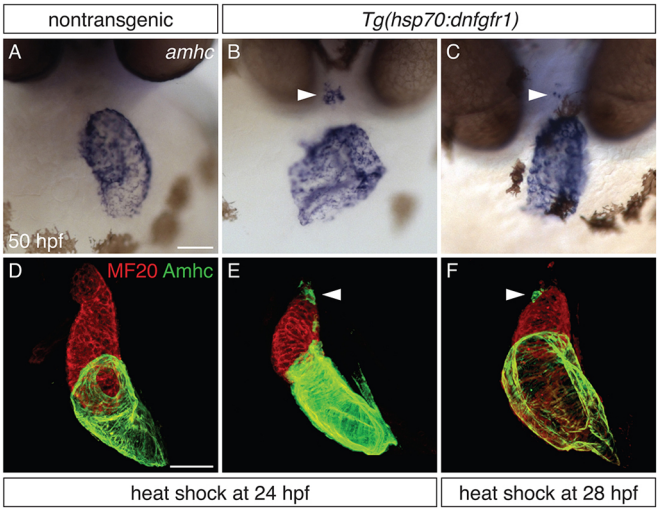

Fig. 2. Defining a time interval during which FGF signaling prevents ectopic *amhc* expression. (A-C) *In situ* hybridization depicts *amhc* expression in frontal views of nontransgenic (A) and *Tg(hsp70:dnfgfr1)* (B,C) embryos at 50 hpf. Heat shock at 24 hpf (A,B) induces ectopic *amhc*-expressing cells in nearly all *Tg(hsp70:dnfgfr1)* embryos (B; *n*=22/24), whereas ectopic cells are induced less frequently with heat shock at 28 hpf (C; *n*=6/36). Heat shock at 18 hpf gives rise to approximately 20-30 ectopic *amhc*-expressing cells (Fig. 1C), heat shock at 24 hpf induces approximately five to ten ectopic *amhc*-expressing cells (B, arrowhead), and approximately two to three ectopic cells are produced with heat shock at 28 hpf (C, arrowhead). (D-F) Three-dimensional reconstructions of immunofluorescence, as in Fig. 1E-H, of nontransgenic (D) and *Tg(hsp70:dnfgfr1)* (E,F) embryos. Whereas *Tg(hsp70:dnfgfr1)* embryos heat shocked at 18 hpf (Fig. 1G) typically display ectopic *amhc*-expressing cells in the ventricular inner curvature and at the arterial pole, *Tg(hsp70:dnfgfr1)* embryos heat shocked at 24 (E) and 28 hpf (F) primarily exhibit ectopic cells at the arterial pole (arrowheads) [*n*=15 for nontransgenic, *n*=10 per condition for *Tg(hsp70:dnfgfr1)*]. Scale bars: 50 µm.

The complementary loss of *vmhc* expression and gain of *amhc* expression in the ventricle of *Tg(hsp70:dnfgfr1)* embryos led us to examine whether these reciprocal changes take place in the same cells. To test this, we examined the dynamics of Amhc and Vmhc protein localization (Fig. 5; Fig. S3). When FGF signaling was reduced, the ventricle contained Vmhc, and not Amhc, at 26 hpf (Fig. 5A-D). However, at 28 hpf, Amhc was detectable within Vmhc^{+} cells located along the inner curvature (Fig. 5E-H). At later stages, Vmhc^{+}Amhc^{+} cells became increasingly prevalent both in the inner curvature and at the arterial pole of the ventricle (Fig. 5I-L), and these cells seemed to exhibit increasingly heightened levels of Amhc (Fig. 5M-P).

The observed patterns of *amhc* and *vmhc* expression (Fig. 4) and Amhc and Vmhc localization (Fig. 5) point to gradual changes in ventricular traits following the loss of FGF signaling. Our results are consistent with a scenario in which reduced FGF signaling causes resident ventricular cardiomyocytes to activate *amhc* expression and to lose *vmhc* expression. Downregulation of *vmhc* is more clearly illustrated through examination of transcripts (Fig. 4I-P), whereas perdurance of Vmhc protein is likely to explain the persistence of Vmhc^{+}Amhc^{+} cells (Fig. 5I-P). Thus, our data suggest that FGF signaling acts to promote the maintenance of ventricular cardiomyocyte characteristics, both by repressing *amhc* expression and by promoting *vmhc* expression. At the same time, these results do not rule out other possible mechanisms through which FGF signaling could prevent the appearance of ectopic *amhc*-expressing cells.

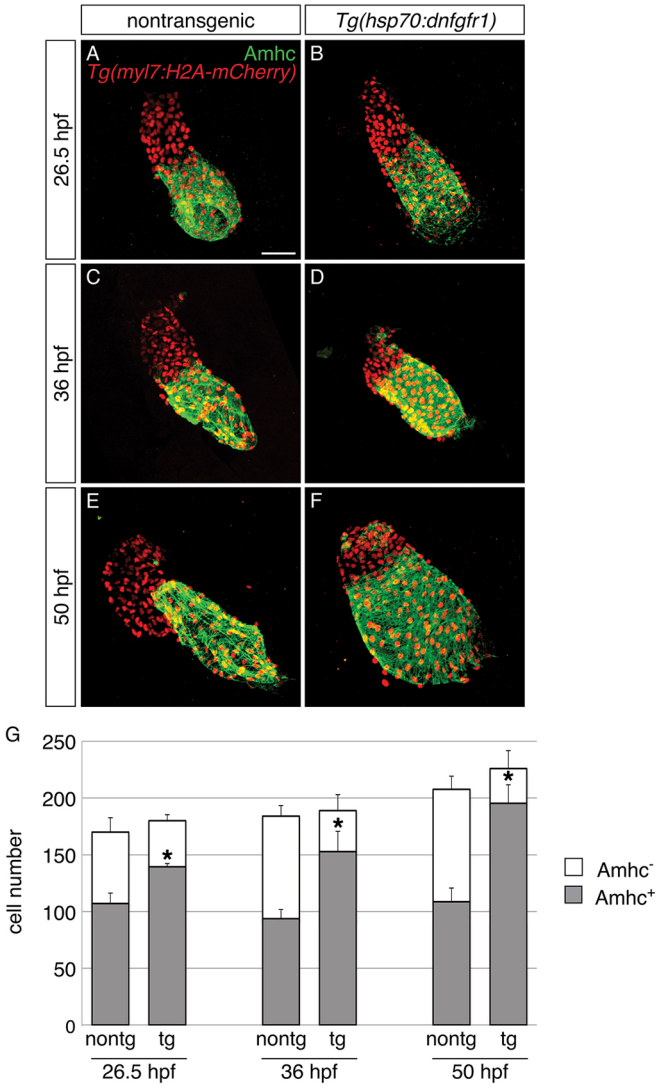

Fig. 3. Progressive accumulation of Amhc^{+} cells and decrease in Amhc^{-} cells in embryos with reduced FGF signaling. (A-F) Immunofluorescence for Amhc (green) and mCherry (red) allows counting of Amhc^{+} and Amhc^{-} cardiomyocytes in nontransgenic (A,C,E) and *Tg(hsp70:dnfgfr1)* embryos (B,D,F) carrying *Tg(myl7:H2A-mCherry)*. Images depict hearts flattened to facilitate visualization of individual myocardial nuclei at 26.5 (A,B), 36 (C,D) and 50 hpf (E,F). Heat-induced expression of *dnfgfr1* at 18 hpf results in a gradual shift in chamber proportions that leads to an enlarged atrium and a reduced ventricle. In addition, there is a visible increase in the presence of Amhc^{+} cells within the ventricle over time. (G) Numbers of Amhc^{+} (gray) and Amhc^{-} (white) cardiomyocytes, as well as the total number of cardiomyocytes (mean+s.d.); asterisks indicate statistically significant differences from nontransgenic (P<0.0001). Cell counts reveal a gradual increase in numbers of Amhc^{+} cells and a corresponding decrease in numbers of Amhc^{-} cells in hearts of *Tg(hsp70:dnfgfr1)* embryos [26.5 hpf: *n*=8 for nontransgenic, *n*=6 for *Tg(hsp70:dnfgfr1)*; 36 hpf: *n*=11 for nontransgenic, *n*=9 for *Tg(hsp70:dnfgfr1)*; 50 hpf: *n*=8 for nontransgenic, *n*=12 for *Tg(hsp70:dnfgfr1)*]. See Table S1 for the number of ectopic Amhc^{+} cells in a subset of these embryos. Scale bar: 50 µm.

Ectopic *amhc*-expressing cells are not derived from the atrium

Some of the ectopic *amhc*-expressing cells in embryos with reduced FGF signaling reside in positions adjacent to the atrium (Figs 1C,D and 4F-H), raising the question of whether any of these cells are derived from atrial cardiomyocytes or from the atrioventricular

Development (2017) 144, 1328-1338 doi:10.1242/dev.143719

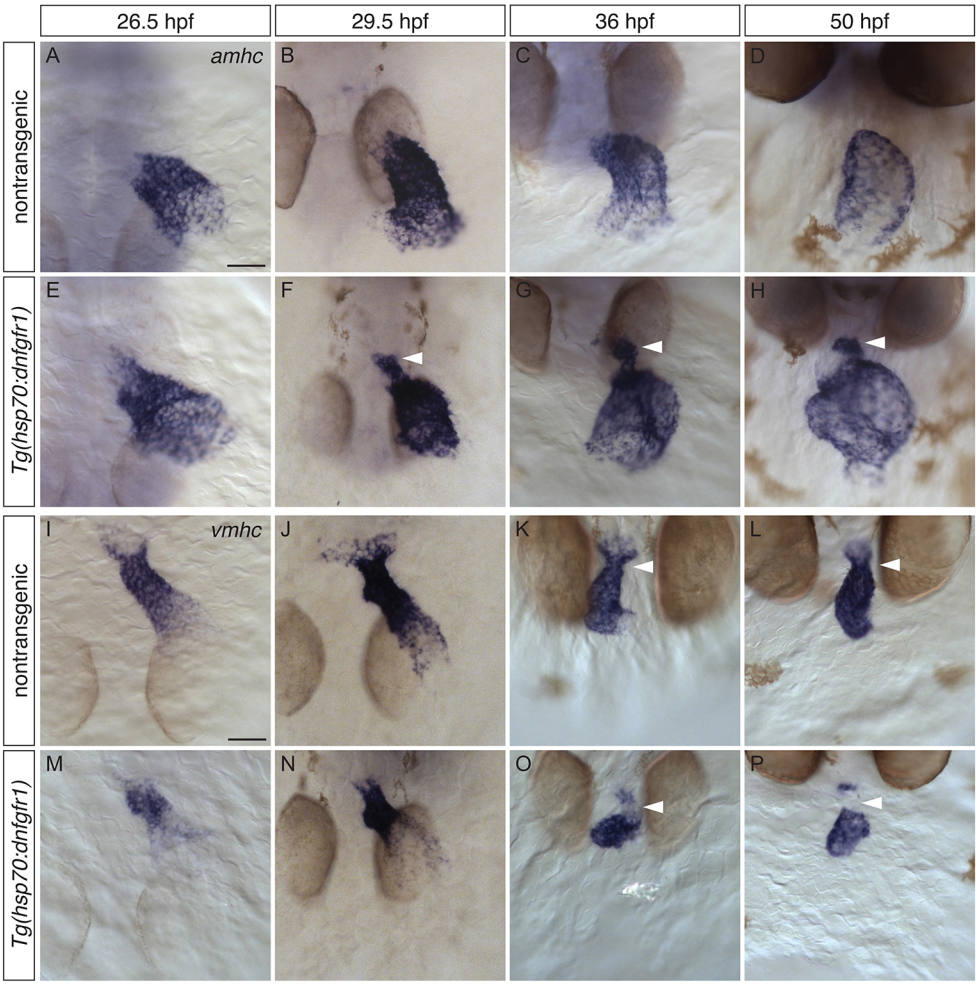

Fig. 4. Increased expression of *amhc* and reduced expression of *vmhc* in the ventricle of embryos with reduced FGF signaling. (A-P) *In situ* hybridization showing *amhc* (A-H) and *vmhc* (I-P) expression in dorsal (A,B,E,F,I,J,M,N) and frontal (C,D,G,H,K,L,O,P) views, following heat shock at 18 hpf. (A-H) In contrast to nontransgenic embryos (A-D), *Tg(hsp70:dnfgfr1)* embryos (E-H) fail to restrict *amhc* to the atrium (n>10 each). (E) At 26.5 hpf, *amhc*-expressing cells can be seen infringing the boundary between the atrium and the ventricle. (F) By 29.5 hpf, *amhc* levels in ectopic cells are upregulated (arrowhead). (G,H) A prominent population of ectopic cells is found at the inner curvature and arterial pole of the ventricle (arrowheads). (I-P) Whereas *vmhc* is robustly expressed in the ventricle of nontransgenic embryos (I-L), this expression pattern is disrupted in *Tg(hsp70:dnfgfr1)* embryos (M-P) (n>10 each). (M,N) At early stages, *Tg(hsp70:dnfgfr1)* embryos display lower levels of *vmhc* expression in regions adjacent to the atrium. (O,P) As development proceeds, *vmhc* levels at the arterial pole become reduced or absent (arrowheads); moreover, the *vmhc* expression pattern appears to be reciprocal to that of ectopic *amhc* in the ventricle. Scale bars: 50 µm.

canal (AVC). Prior studies have demonstrated that injury to the larval ventricle can cause atrial cardiomyocytes to transdifferentiate into ventricular cardiomyocytes in order to replenish the damaged tissue (Zhang et al., 2013). To test the possibility that a similar mechanism recruits cells from the atrium into the ventricle when FGF signaling is inhibited, we labeled *amhc*-expressing cells and followed them over time. To do so, we generated transgenic lines carrying a photoconvertible reporter, *Tg(amhc:dendra)* (Fig. S4), which expresses the fluorescent protein Dendra under the control of a previously characterized *amhc* promoter (Zhang et al., 2013).

To analyze whether ectopic *amhc*-expressing cells in the ventricle originate from the atrium or the AVC, we exposed *Tg(amhc:dendra)* embryos to SU5402 at 18 hpf, performed photoconversion at 26 hpf, and evaluated the fluorescence of the ectopic *amhc*-expressing cells at 48 hpf (Fig. 6). We chose to perform photoconversion at 26 hpf because the ventricle of SU5402-treated embryos is typically devoid of *amhc* expression at this stage (Fig. S4C,D); moreover, Dendra fluorescence in *Tg(amhc:dendra)* embryos is robust enough at 26 hpf to ensure successful detection of its photoconverted red form at the experimental endpoint (Fig. S4A,B). In DMSO-treated control embryos, Dendra was found only in the atrium, and atrial cells exhibited both green and red fluorescence (Fig. 6A-D). In contrast, SU5402-treated embryos contained Dendra both in the atrium and in groups of ectopic cells within the ventricle (Fig. 6E-L). In all of the SU5402-treated embryos examined (n=15), we identified Dendra$^+$ cells in the ventricular inner curvature or at the arterial pole that displayed green, but not red, fluorescence, indicating that these cells had not been expressing *amhc* at the time of photoconversion. In the majority of these embryos (n=10/15), all of the Dendra$^+$ cells seen in the inner curvature and at the arterial pole exhibited only green fluorescence (Fig. 6E-L). However, in a few embryos (n=5/15), the observed group of green-only Dendra$^+$ cells was accompanied by one to three doubly fluorescent Dendra$^+$ cells. These relatively rare examples of doubly fluorescent Dendra$^+$ cells probably represent cases in which a few cells had already initiated ectopic *amhc* expression at the time of photoconversion. Altogether, our data indicate that the vast majority of the ectopic *amhc*-expressing cells induced by loss of FGF signaling are not derived from *amhc*-expressing cells in the atrium or AVC.

FGF signaling inhibits *amhc* expression in both early-differentiating and late-differentiating ventricular cardiomyocytes

As some of the ectopic *amhc*-expressing cells in embryos with reduced FGF signaling reside near the arterial pole, we wondered whether any of these might be derived from the late-differentiating second heart field (SHF) progenitor cells that normally construct this portion of the ventricle (de Pater et al., 2009; Hami et al., 2011; Lazic and Scott, 2011; Zhou et al., 2011). If so, this would parallel a previous finding in *nkx2.5* mutants, in which some of the ectopic *amhc*-expressing cells in the ventricle are late-differentiating

Development (2017) 144, 1328-1338 doi:10.1242/dev.143719

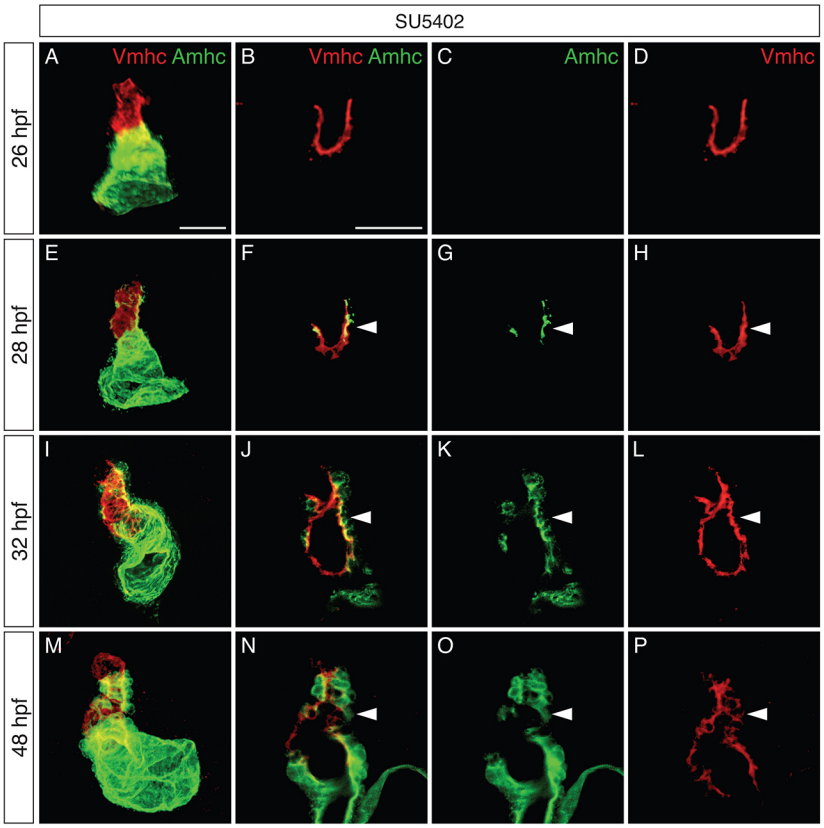

Fig. 5. Increased colocalization of Vmhc and Amhc in the ventricle when FGF signaling is inhibited. (A-P) Immunofluorescence showing Vmhc (red) and Amhc (green) localization in embryos treated with SU5402 from 18 hpf. Lateral views are three-dimensional reconstructions (A,E,I,M) or magnified single optical sections, showing both channels (B,F,J,N), green only (C,G,K,O) or red only (D,H,L,P). See Fig. S3 for DMSO-treated control embryos. (A-D) At 26 hpf, the SU5402-treated ventricle contains only Vmhc (n=10). (E-H) By 28 hpf, Amhc is evident within some Vmhc$^+$ cells, particularly along the inner curvature (arrowheads; n=9). We presume that these cells are early-differentiating cardiomyocytes, as late-differentiating cardiomyocytes normally contribute to the heart after 30 hpf (Lazic and Scott, 2011). (I-L) By 32 hpf, increasing numbers of Amhc$^+$Vmhc$^+$ cells are visible in the ventricle (arrowheads; n=11). (M-P) By 48 hpf, higher levels of Amhc accumulate in ectopic cells (arrowheads), in concert with diminishing levels of Vmhc (n=9). Scale bars: 50 µm.

cardiomyocytes (George et al., 2015). To begin investigating whether FGF signaling influences ventricular characteristics in late-differentiating cells, we first examined whether SHF progenitor cells were present in embryos subjected to our experimental conditions. Prior studies have shown that strong inhibition of FGF signaling with a high dose of SU5402 (10 µM) beginning at 24 hpf can nearly eliminate the formation of *mef2cb*-expressing SHF progenitor cells (Lazic and Scott, 2011; Zeng and Yelon, 2014). However, our strategies for reduction of FGF signaling at 18 hpf, either by heat shock of *Tg(hsp70:dnfgfr1)* embryos or by exposure

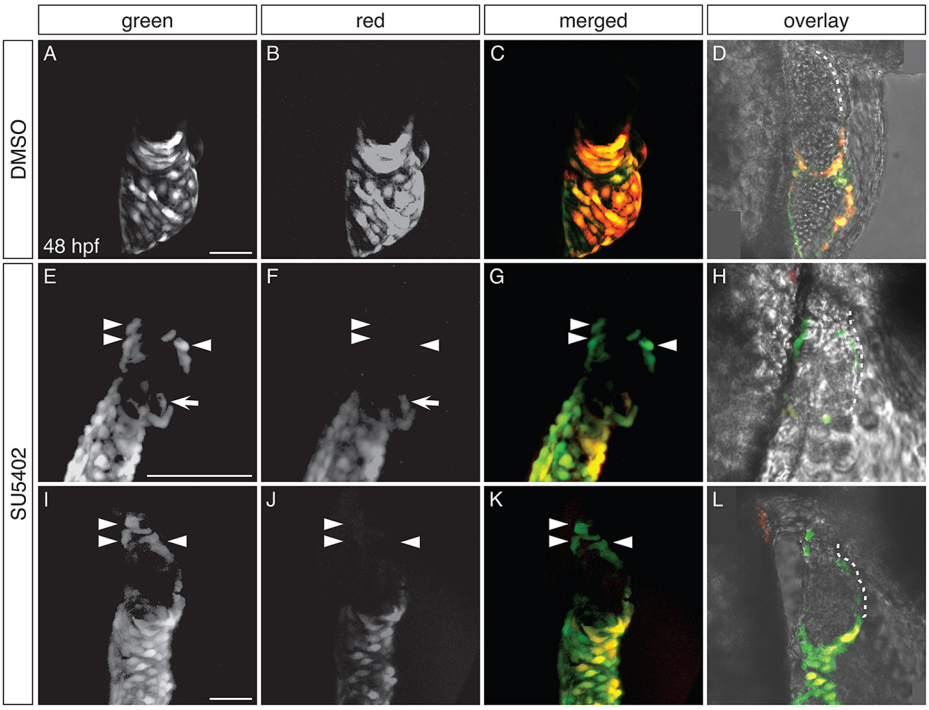

Fig. 6. Ectopic *amhc*-expressing cells are not derived from the atrium or AVC. (A-L) Dendra fluorescence in live DMSO-treated (A-D) and SU5402-treated (E-L) *Tg(amhc:dendra)* embryos at 48 hpf, following photoconversion at 26 hpf; two representative SU5402-treated embryos are shown. Images are three-dimensional reconstructions (A-C,E-G,I-K) or single optical sections (D,H,L); lateral views, anterior to the right. (D,H,L) Overlay illustrates location of Dendra$^+$ cells within the heart; white dashes outline the ventricle. See Fig. S4 for additional information regarding experimental design. (A-D) In DMSO-treated controls, Dendra is found only in the atrium and AVC. Both green and red forms of Dendra are visible, as illustrated in single channel and merged views (n=10). (E-L) SU5402-treated embryos exhibit Dendra$^+$ cells in the ventricle, in distinct clusters at the arterial pole and in the inner curvature (arrowheads). Cells at the arterial pole and inner curvature fluoresce green, but not red (arrowheads; n=15). Dendra$^+$ cells are also found in and near the AVC (arrows), as seen in controls (A-D), reflecting the wild-type expression of *amhc* in this area (Foglia et al., 2016). Scale bars: 50 µm (A,I); 100 µm (E).

Development (2017) 144, 1328-1338 doi:10.1242/dev.143719

to a lower dose of SU5402 (5 µM), did not affect *mef2cb* expression in the SHF progenitor population (Fig. S5; data not shown). In addition, as in control embryos (Fig. 7A-D), SHF progenitor cells went on to contribute late-differentiating cardiomyocytes to the arterial pole in *Tg(hsp70:dnfgfr1)* embryos (Fig. 7E-H), as shown by an established developmental timing assay that can distinguish early-differentiating from late-differentiating cardiomyocytes (de Pater et al., 2009).

To test whether ectopic *amhc*-expressing cells at the arterial pole represent early-differentiating or late-differentiating cardiomyocytes, we performed an adapted developmental timing assay that employs the transgenes *Tg(myl7:dsredt4)* and *Tg(amhc:egfp)*. In control embryos expressing these transgenes at 48 hpf, eGFP is found in the atrium, and DsRed is found in early-differentiating, but not late-differentiating, cardiomyocytes (Fig. 8A-D). In contrast, when FGF signaling is reduced, eGFP is found both in the atrium and ectopically in the ventricle (Fig. 8E-L). In all of the SU5402-treated embryos examined (n=10), the ventricle contained eGFP$^+$DsRed$^+$ cardiomyocytes (Fig. 8E-L, arrows), which we categorized as early-differentiating. In addition, the majority of these embryos (n=7/10) also contained some eGFP$^+$ cells at the arterial pole that lacked DsRed and were therefore categorized as late-differentiating (Fig. 8E-L, arrowheads).

Synthesizing all of our data, we propose that both early-differentiating and late-differentiating ventricular cardiomyocytes can become ectopic *amhc*-expressing cells when FGF signaling is reduced. In addition to the results from our developmental timing assay (Fig. 8E-L), the locations of the observed ectopic cells are consistent with their derivation from both of these populations. Late-differentiating cardiomyocytes populate the arterial pole (de Pater et al., 2009; Hami et al., 2011; Lazic and Scott, 2011; Zhou et al., 2011), whereas early-differentiating cells construct the inner curvature (de Pater et al., 2009; Zhou et al., 2011), and we routinely found ectopic *amhc* expression in each of these areas (e.g. Fig. 8E-L). We also found ectopic *amhc*-expressing cells in the proximal portion of the ventricle (e.g. Fig. 8E), another early-differentiating territory (de Pater et al., 2009). Notably, ectopic *amhc*-expressing cells in this region were also evident in a separate set of experiments in which we mosaically expressed the *Tg(hsp70:dnfgfr1)* construct in clusters of ventricular cardiomyocytes: in these mosaics, *dnfgfr1*-expressing cells in the proximal ventricle were found to be Amhc$^+$ (Fig. 8M-P). The time frame during which we observed the appearance of ectopic *amhc*-expressing cells also fits with the timing of the early and late phases of ventricular differentiation: in embryos with reduced FGF signaling, we could first detect ectopic Amhc within Vmhc$^+$ cells in the early-differentiating inner curvature as early as 28 hpf (e.g. Fig. 5E-H), whereas more ectopic cells appeared at the arterial pole after 30 hpf (e.g. Fig. 5I-L), when late-differentiating cells are typically added (Lazic and Scott, 2011). Taken together, our results suggest that FGF signaling plays important and similar roles in both populations of ventricular cells: the FGF pathway represses atrial traits and maintains ventricular characteristics in both early-differentiating and late-differentiating cardiomyocytes.

FGF signaling functions upstream of Nkx genes to repress ectopic *amhc* expression

In embryos with reduced FGF signaling, as in embryos lacking Nkx transcription factors (George et al., 2015; Targoff et al., 2013), we observe gradual diminishment of the ventricle, gradual enlargement of the atrium, and the appearance of ectopic *amhc* expression in both early-differentiating and late-differentiating ventricular cardiomyocytes. These similarities suggest that FGF signaling and Nkx genes play comparable roles in the maintenance of ventricular identity. In addition, we found that treatment with a low dose of SU5402 (4 µM) can subtly enhance the appearance of ectopic *amhc* expression in *nkx2.5* mutant embryos (Fig. S6), suggesting that FGF signaling and Nkx genes operate in the same pathway.

As FGF signaling has been shown to promote *nkx2.5* expression in the anterior lateral plate mesoderm of the early embryo (Alsan and Schultheiss, 2002; Keren-Politansky et al., 2009; Reifers et al., 2000; Simões et al., 2011), we examined the expression of *nkx2.5* and *nkx2.7* in the hearts of embryos with reduced FGF signaling. In contrast to control siblings, cardiac expression of *nkx2.5* and *nkx2.7* was reduced within the ventricle of *Tg(hsp70:dnfgfr1)* embryos following heat shock at 18 hpf (Fig. 9A-D). As *nkx2.5* and *nkx2.7* expression are established prior to 18 hpf (Lee et al., 1996), these results suggest that FGF signaling is required to maintain expression of Nkx genes.

To test the hypothesis that FGF signaling functions upstream of Nkx genes to prevent ventricular expression of *amhc*, we examined whether overexpression of *nkx2.5* can inhibit the formation of ectopic *amhc*-expressing cells in embryos with reduced FGF signaling. We employed a previously characterized transgene, *Tg(hsp70l:nkx2.5-EGFP)* [abbreviated as *Tg(hsp70:nkx2.5)*] (George et al., 2015), to induce *nkx2.5* expression. Prior studies using this transgene have shown that overexpression of *nkx2.5* can rescue the defects in chamber proportionality and repress ectopic *amhc* expression in *nkx2.5* mutants (George et al., 2015). In our experiments, *Tg(hsp70:nkx2.5)* embryos were treated with SU5402 from 18 hpf and subsequently heat shocked at 24 hpf. We found that 84% (65/77) of nontransgenic embryos treated with SU5402 had ectopic *amhc*-expressing cells, whereas only 64% (74/119) of *Tg(hsp70:nkx2.5)* embryos exhibited any ectopic *amhc* expression (Fig. 9E-H). This decrease in the frequency of detecting ectopic *amhc* expression, although modest, is statistically significant (P=0.0019, Fisher's exact test) and seems to represent a partial rescue of the SU5402-treated phenotype. Therefore, our results suggest that FGF signaling functions upstream of *nkx2.5* in a pathway that ensures the maintenance of ventricular identity.

DISCUSSION

Taken together, our data demonstrate that the FGF signaling pathway plays a crucial role in maintaining the characteristics of the developing ventricle. We propose a model in which FGF signaling acts to reinforce the assignment of ventricular identity, both by repressing expression of atrial genes and by promoting expression of ventricular genes. For early-differentiating cells, FGF signaling is required to maintain the appropriate number of cardiomyocytes in the ventricle, as well as to preserve the ventricular characteristics of these cells. For late-differentiating cells, FGF signaling is required to promote their accretion to the arterial pole (de Pater et al., 2009; Lazic and Scott, 2011; Marques et al., 2008; Zeng and Yelon, 2014), as well as to regulate their presentation of appropriate ventricular traits. Thus, sustained FGF signaling suppresses myocardial plasticity and preserves the integrity of the ventricular chamber.

Our studies provide several new insights regarding the nature of ventricular plasticity and commitment. Beyond defining a new role for FGF signaling in enforcing ventricular character, our work has also shed light on the spatial distribution and temporal limitations of ventricular plasticity. Spatially, our results reveal that distinct regions within the ventricle are differentially susceptible to the loss

Development (2017) 144, 1328-1338 doi:10.1242/dev.143719

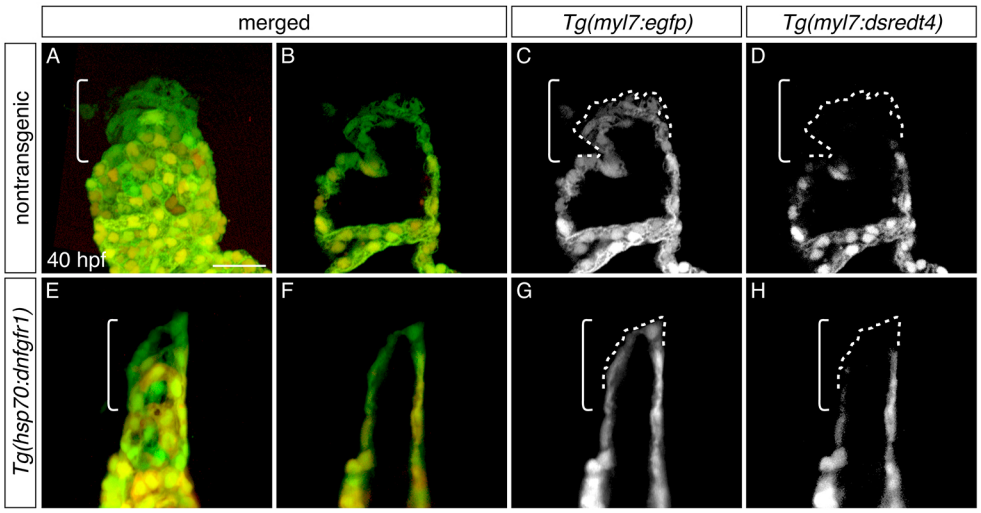

Fig. 7. Late-differentiating cardiomyocytes contribute to the heart after inhibition of FGF signaling. (A-H) Three-dimensional reconstructions (A,E) and single optical sections (B-D,F-H) of live embryos carrying *Tg(myl7:egfp)* and *Tg(myl7:dsredt4)*; lateral views at 40 hpf, after heat shock at 18 hpf. Owing to the differential protein-folding kinetics of eGFP and dsRed (Lepilina et al., 2006), reporter transgene expression distinguishes early-differentiating ($eGFP^+dsRed^+$) and late-differentiating cardiomyocytes ($eGFP^+dsRed^-$) (de Pater et al., 2009). As in nontransgenic embryos (A-D, *n*=6), late-differentiating cardiomyocytes ($eGFP^+dsRed^-$, dashed outlines) contribute to the arterial pole (brackets) in *Tg(hsp70:dnfgfr1)* embryos (E-H; *n*=8). Scale bar: 30 µm.

of FGF signaling: for example, we more frequently observe ectopic *amhc*-expressing cells in the inner curvature than in the outer curvature of the ventricle. This differential distribution could signify spatial heterogeneity in the degree to which cells are committed to the ventricular differentiation pathway, with the more primitive myocardium of the inner curvature being more malleable than the working myocardium of the outer curvature. Perhaps commonalities in the programs of gene expression within the inner curvature and within the arterial pole underlie their similar dependence on sustained FGF signaling. Temporally, our data indicate a defined time window during which the ventricular myocardium is vulnerable to the effects of reduced FGF signaling. Together with

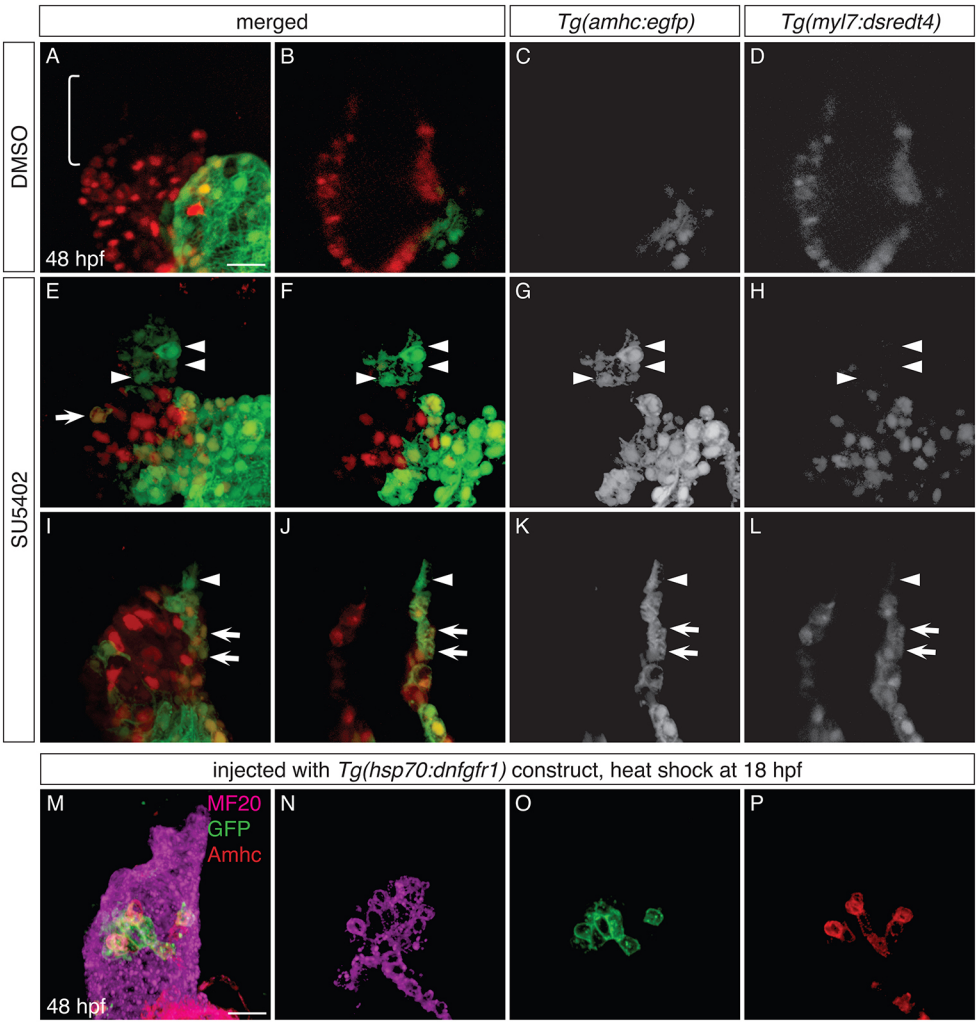

Fig. 8. FGF signaling influences the identity of both early-differentiating and late-differentiating ventricular cardiomyocytes. (A-L) Three-dimensional reconstructions (A,E,I) and single optical sections (B-D,F-H,J-L) of live *Tg(amhc:egfp)*;*Tg(myl7:dsredt4)* embryos; lateral views at 48 hpf, after exposure to DMSO (A-D) or SU5402 (E-L) from 18 hpf. (A-D) As expected, control embryos display eGFP in the atrium and not in the ventricle, and the arterial pole (bracket) is composed of late-differentiating cardiomyocytes ($DsRed^-$) (*n*=5). (E-L) In SU5402-treated embryos, eGFP is routinely found in the ventricle (*n*=10). Two representative embryos (E-H and I-L) illustrate detection of eGFP both in early-differentiating cardiomyocytes (arrows, $eGFP^+DsRed^+$; *n*=10/10) and in late-differentiating cardiomyocytes (arrowheads, $eGFP^+DsRed^-$; *n*=7/10). (M-P) Immunofluorescence for MF20 (magenta), GFP (green) and Amhc (red) at 48 hpf indicates mosaic expression of *dnfgfr1-egfp* in the ventricle of an embryo that was injected with the *Tg(hsp70:dnfgfr1)* construct and then heat shocked at 18 hpf; three-dimensional reconstruction (M) and single optical sections (N-P). The *dnfgfr1-egfp*-expressing cells in the proximal ventricle exhibit variegated levels of Amhc (P; *n*=3). Scale bars: 30 µm.

Development (2017) 144, 1328-1338 doi:10.1242/dev.143719

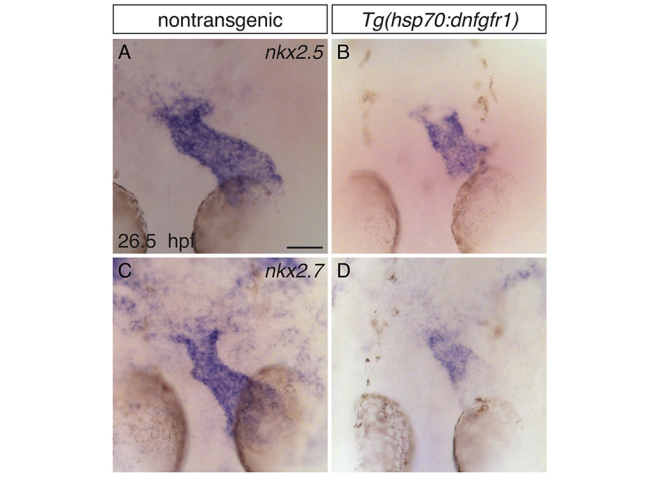

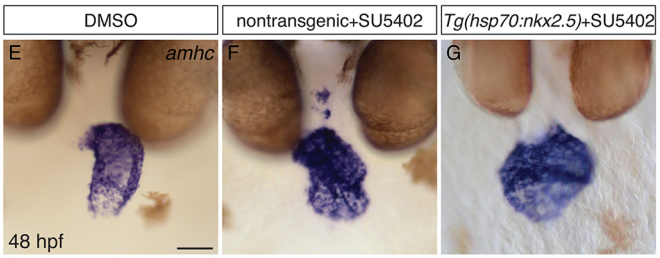

H

Condition	Number of embryos with ectopic *amhc*	Total number of embryos	% embryos with ectopic *amhc*
nontransgenic	65	77	84%
Tg(hsp70:nkx2.5)	76	119	64% *

Fig. 9. FGF signaling functions upstream of Nkx genes to repress *amhc* expression in the ventricle. (A-D) *In situ* hybridization showing *nkx2.5* (A,B) and *nkx2.7* (C,D) expression in dorsal views at 26.5 hpf, following heat shock at 18 hpf. Nontransgenic embryos (A,C) exhibit robust expression of *nkx2.5* (*n*=24) and *nkx2.7* (*n*=12), and *Tg(hsp70:dnfgfr1)* embryos (B,D) exhibit reduced expression of *nkx2.5* (*n*=24) and *nkx2.7* (*n*=12). This reflects a reduced amount of ventricular tissue in *Tg(hsp70:dnfgfr1)* embryos (compare with Fig. 4M), as well as lower expression levels within this tissue. (E-G) *In situ* hybridization showing *amhc* expression at 48 hpf in nontransgenic (F) and *Tg(hsp70:nkx2.5)* (E,G) embryos treated with DMSO (E) or SU5402 (F,G); frontal views. In some cases (G), overexpression of *nkx2.5* represses ectopic *amhc* expression in *Tg(hsp70:nkx2.5)* embryos that were treated with SU5402 at 18 hpf and subsequently heat shocked at 24 hpf. (H) Table reports the results of experiments gauging whether *amhc* expression in the ventricle of SU5402-treated embryos can be repressed by overexpression of *nkx2.5*. Asterisk indicates a statistically significant difference in the frequency of detecting ectopic *amhc* expression, compared to nontransgenic siblings (P=0.0019, Fisher's exact test), representing partial rescue of the SU5402-treated phenotype. The degree of rescue was not enhanced when we used embryos carrying two copies of *Tg(hsp70:nkx2.5)* or when we administered two rounds of heat shock (data not shown). Scale bars: 50 µm.

prior studies that indicate that *nkx2.5* acts to maintain ventricular identity during a similar time frame (George et al., 2015), these findings might reflect the timing of a transition from plasticity to commitment within the ventricular myocardium. Similarly, a recent study in *Xenopus* suggested that ventricular fate can be influenced over a relatively broad time window and that the responsiveness of ventricular precursors to inductive signals is gradually lost over time (Caporilli and Latinkic, 2016). In future studies, it will be intriguing to seek the differences in gene expression that presumably underlie the spatial heterogeneity and temporal progression of commitment to a ventricular identity.

In addition, our work adds a new facet to our understanding of SHF development. Numerous studies have focused on the signaling pathways that regulate the production, proliferation or differentiation of SHF-derived progenitor cells (e.g. de Pater et al., 2009; Dyer and Kirby, 2009; Ilagan et al., 2006; Lazic and Scott, 2011; Park et al., 2006; Tirosh-Finkel et al., 2010; Zeng and Yelon, 2014; Zhou et al., 2011), but the signals that confer the appropriate chamber-specific characteristics to these late-differentiating cells have not been characterized. Strikingly, we find that reduction of FGF signaling causes late-differentiating cells to initiate *amhc* expression inappropriately, suggesting either misassignment to an atrial identity or failure to maintain the ventricular differentiation program. Thus, our analysis of FGF signaling provides the first demonstration of a pathway that plays a key role in enforcing ventricular identity in late-differentiating cardiomyocytes.

We note that our studies rely on the expression of *vmhc* and *amhc* as proxies for ventricular and atrial identity. Even though neither of these genes is strictly chamber specific (Berdougo et al., 2003; Foglia et al., 2016; Yelon et al., 1999), they serve here as representatives of larger gene expression programs in the ventricle and the atrium. It would be interesting to evaluate whether the ectopic *amhc*-expressing cells in the ventricle also express additional atrial genes; unfortunately, *amhc* is the most robust marker of its type that is currently available. The mechanisms regulating *vmhc* and *amhc* expression are undoubtedly relevant to the control of chamber identity, but it will also be valuable for future studies to expand the roster of ventricular and atrial markers and thereby extend our comprehension of the breadth of influence of FGF signaling.

We envisage a pathway in which FGF signaling acts upstream of Nkx genes, which in turn regulate the downstream effectors *irx4* and *hey2* (Targoff et al., 2013). Our findings regarding the function of FGF signaling in both early-differentiating and late-differentiating ventricular cardiomyocytes echo what has previously been observed in zebrafish Nkx-deficient embryos (George et al., 2015; Targoff et al., 2013). Moreover, our data suggest that FGF signaling acts through *nkx2.5* to execute its function in repressing ectopic *amhc* expression. However, although we observed a statistically significant improvement in SU5402-treated embryos upon overexpression of *nkx2.5*, this result represents only a partial rescue. One possible explanation for this outcome is that we are failing to induce the level of *nkx2.5* expression that is required for thorough repression of ectopic *amhc*. Alternatively, perhaps both *nkx2.5* and *nkx2.7* are required to prevent ectopic *amhc* expression. Because these two genes are not entirely redundant in function (George et al., 2015), overexpression of *nkx2.5* might not be able to compensate for reduced activity of both. Lastly, FGF signaling might act through additional downstream effector genes, beyond *nkx2.5* and *nkx2.7*, to repress ectopic *amhc* and maintain ventricular identity. Identification of these putative downstream effectors of the FGF pathway, as well as elucidation of the mechanism through which FGF signaling promotes Nkx gene expression, will be important future endeavors.

More broadly, our insights into the signaling pathways that reinforce chamber identity have important implications for approaches to cardiac regenerative medicine. Efforts towards the *in vitro* differentiation of homogeneous populations of mature cardiomyocytes are moving increasingly towards protocols that employ cocktails of small molecules to manipulate signaling pathways and modify chromatin (e.g. Cao et al., 2016). As these protocols are further refined, it will be crucial to control not only the pathways that direct chamber-specific lineage decisions but also the

Development (2017) 144, 1328-1338 doi:10.1242/dev.143719

pathways that reinforce commitment to chamber identity. Our work suggests that regulation of the FGF signaling pathway will be an important element of future regenerative medicine strategies that aim to harness the inherent plasticity of ventricular cardiomyocytes.

MATERIALS AND METHODS

Zebrafish

We used the following zebrafish strains: *Tg(hsp70l:dnfgfr1-EGFP)*^{pd1} (Lee et al., 2005), *Tg(hsp70:ca-fgfr1)*^{pd3} (Marques et al., 2008), *Tg(amhc:egfp)*^{s958} (Zhang et al., 2013), *Tg(myl7:H2A-mCherry)*^{sd12} (Schumacher et al., 2013), *Tg(myl7:egfp)*^{twu277} (Huang et al., 2003), *Tg(myl7:dsredt4)*^{sk74} (Garavito-Aguilar et al., 2010), *Tg(hsp70l:nkx2.5-EGFP)*^{fcu1} (George et al., 2015), *nkx2.5*^{vu179} (Targoff et al., 2013) and *fgf8a*^{ti282a} (Reifers et al., 1998). The *fgf8a*^{ti282a} mutation alters splicing and might not be a null allele, as low levels of wild-type transcript can be detected in mutant embryos (Reifers et al., 1998). All zebrafish work followed Institutional Animal Care and Use Committee-approved protocols.

Immunofluorescence and *in situ* hybridization

Whole-mount immunofluorescence was performed as previously described (Alexander et al., 1998), using the antibodies in Table S2. Previously described protocols were also used for *in situ* hybridization (Thomas et al., 2008) and fluorescence *in situ* hybridization in combination with immunofluorescence (Zeng and Yelon, 2014), using established probes for *amhc* (*myh6*; ZDB-GENE-031112-1), *vmhc* (ZDB-GENE-991123-5), *myl7* (ZDB-GENE-991019-3), *nkx2.5* (ZDB-GENE-980526-321), *nkx2.7* (ZDB-GENE-990415-179) and *mef2cb* (ZDB-GENE-04901-7). All data represent at least two technical replicates of each experiment.

Cardiomyocyte counting

To count cardiomyocytes in Fig. 3, we employed embryos carrying the transgenes *Tg(hsp70l:dnfgfr1-EGFP)* and *Tg(myl7:H2A-mCherry)*. We counted both Amhc^{+} and Amhc^{-} cardiomyocyte nuclei using an established protocol (Schoenebeck et al., 2007) and employed a two-tailed, unpaired *t*-test to compare data sets. To estimate the numbers of ectopic *amhc*-expressing cells in Figs 1 and 2, we scored morphologically evident cells in which the NBT/BCIP precipitate surrounded a presumed nucleus, as in prior studies (Thomas et al., 2008).

Photoconversion

To generate *Tg(amhc:dendra)*, we placed the Dendra coding sequence downstream of the previously characterized *amhc* promoter (Zhang et al., 2013). Transgenic founders were established using standard techniques for I-SceI-mediated transgenesis (Soroldoni et al., 2009). F1 and F2 progeny of two different founders with comparable expression levels were used.

We treated *Tg(amhc:dendra)* embryos with either SU5402 or DMSO at 18 hpf, and subsequently performed photoconversion at 26 hpf through exposure to a series of 30 s intervals of UV light, using a DAPI filter set on a Zeiss Axioimager microscope. Exposure continued for up to 120 s, until all *Tg(amhc:dendra)*-expressing cells exhibited red fluorescence. Embryos were maintained in either SU5402 or DMSO until 48 hpf.

Imaging

Images were captured using a Zeiss Axioimager and Axiocam and were processed using Zeiss Axiovision and Adobe Creative Suite software. Confocal imaging was performed with a Leica SP5 confocal laser-scanning microscope and analyzed using Imaris software (Bitplane).

Heat shock

Embryos from outcrosses of fish heterozygous for *Tg(hsp70l:dnfgfr1-EGFP)*, *Tg(hsp70l:ca-fgfr1)* or *Tg(hsp70l:nkx2.5-EGFP)* were kept at 28.5°C prior to heat shock. To perform heat shock, embryos were added to 500 ml of E3, pre-equilibrated to 37.5°C. *Tg(hsp70l:dnfgfr1-EGFP)* clutches were incubated at 37.5°C for 22 min; in most of our experiments with this transgene, we administered heat shock at 18 hpf, because treatment at this time point proved to be the most potent (Figs 1 and 2). *Tg(hsp70l:ca-fgfr1)* clutches were incubated at 37.5°C for 60 min at 18 hpf. Rescue experiments were conducted by first treating *Tg(hsp70l:nkx2.5-EGFP)* embryos with SU5402 at 18 hpf, followed by heat shock at 24 hpf at 37.5°C for 60 min.

Following heat shock, embryos carrying *Tg(hsp70l:dnfgfr1-EGFP)* or *Tg(hsp70l:nkx2.5-EGFP)* were identified by eGFP induction, and embryos carrying *Tg(hsp70l:ca-fgfr1)* were identified by red fluorescence in the lens. For all experiments employing heat shock, nontransgenic siblings served as controls.

SU5402

SU5402 treatments were performed as previously described (Marques et al., 2008). A 10 mM stock of SU5402 (Tocris and Sigma) in DMSO was diluted to a working concentration of 5 µM in E3 medium. Control embryos were treated with a corresponding dilution of DMSO in E3. Up to 12 embryos were housed in 1 ml in a glass vial.

We chose to use 5 µM SU5402 after comparing the effects of a range of doses. This concentration caused a consistent cardiac phenotype without notable toxicity. Higher concentrations were more potent and led to Amhc being found throughout the heart, consistent with prior observations (Reifers et al., 2000), but these doses also caused considerable embryonic toxicity.

In all assays performed, SU5402 treatment and heat-induced expression of *dnfgfr1* produced comparable results. However, *Tg(hsp70l:dnfgfr1-EGFP)* embryos were used whenever possible, because they exhibited a more consistent phenotype. In some experiments (Figs 5, 6 and 8A-L), we took advantage of SU5402 treatments in order to avoid complications resulting from perdurance of the GFP reporter within *Tg(hsp70l:dnfgfr1-EGFP)*.

Mosaic expression

For mosaic studies, wild-type embryos at the one-cell stage were injected with 30 pg of *Tg(hsp70l:dnfgfr1-EGFP)* (Lee et al., 2005) plasmid. Embryos were heat shocked at 18 hpf and fixed for immunofluorescence at 48 hpf.

Acknowledgements

We thank K. Cooper, S.A. Wasserman, and members of the Yelon laboratory for thoughtful input.

Competing interests

The authors declare no competing or financial interests.

Author contributions

A.P. and D.Y. designed these studies; A.P., X.-X.I.Z., P.S., S.R.M. and D.Y. performed experiments; V.G., K.L.T. and N.C.C. generated reagents; A.P. and D.Y. analyzed the data; and A.P. and D.Y. wrote the manuscript with input from all authors.

Funding

This work was supported by grants from the National Institutes of Health [R01HL069594 and R01HL108599 to D.Y.; K12HD043389, K08HL088002 and R01HL131438 to K.L.T.] and from the American Heart Association [15IRG22730014 to D.Y.]. Deposited in PMC for release after 12 months.

Supplementary information

Supplementary information available online at
http://dev.biologists.org/lookup/doi/10.1242/dev.143719.supplemental

References

Abu-Issa, R., Smyth, G., Smoak, I., Yamamura, K. and Meyers, E. N. (2002). Fgf8 is required for pharyngeal arch and cardiovascular development in the mouse. *Development* **129**, 4613-4625.

Alexander, J., Stainier, D. Y. R. and Yelon, D. (1998). Screening mosaic F1 females for mutations affecting zebrafish heart induction and patterning. *Dev. Genet.* **22**, 288-299.

Alsan, B. H. and Schultheiss, T. M. (2002). Regulation of avian cardiogenesis by Fgf8 signaling. *Development* **129**, 1935-1943.

Bao, Z. Z., Bruneau, B. G., Seidman, J. G., Seidman, C. E. and Cepko, C. L. (1999). Regulation of chamber-specific gene expression in the developing heart by Irx4. *Science* **283**, 1161-1164.

Development (2017) 144, 1328-1338 doi:10.1242/dev.143719

Barth, A. S., Merk, S., Arnoldi, E., Zwermann, L., Kloos, P., Gebauer, M., Steinmeyer, K., Bleich, M., Kääb, S., Pfeufer, A. et al. (2005). Functional profiling of human atrial and ventricular gene expression. *Pflug. Arch. Eur. J. Phy.* **450**, 201-208.

Berdougo, E., Coleman, H., Lee, D. H., Stainier, D. Y. and Yelon, D. (2003). Mutation of weak atrium/atrial myosin heavy chain disrupts atrial function and influences ventricular morphogenesis in zebrafish. *Development* **130**, 6121-6129.

Bisaha, J. G. and Bader, D. (1991). Identification and characterization of a ventricular-specific avian myosin heavy-chain, Vmhc1-expression in differentiating cardiac and skeletal-muscle. *Dev. Biol.* **148**, 355-364.

Bruneau, B. G., Bao, Z.-Z., Tanaka, M., Schott, J.-J., Izumo, S., Cepko, C. L., Seidman, J. G. and Seidman, C. E. (2000). Cardiac expression of the ventricle-specific homeobox gene Irx4 is modulated by Nkx2-5 and dHand. *Dev. Biol.* **217**, 266-277.

Bruneau, B. G., Bao, Z.-Z., Fatkin, D., Xavier-Neto, J., Georgakopoulos, D., Maguire, C. T., Berul, C. I., Kass, D. A., Kuroski-de Bold, M. L., de Bold, A. J. et al. (2001). Cardiomyopathy in Irx4-deficient mice is preceded by abnormal ventricular gene expression. *Mol. Cell. Biol.* **21**, 1730-1736.

Cao, N., Huang, Y., Zheng, J. S., Spencer, C. I., Zhang, Y., Fu, J.-D., Nie, B. M., Xie, M., Zhang, M. L., Wang, H. X. et al. (2016). Conversion of human fibroblasts into functional cardiomyocytes by small molecules. *Science* **352**, 1216-1220.

Caporilli, S. and Latinkic, B. V. (2016). Ventricular cell fate can be specified until the onset of myocardial differentiation. *Mech. Dev.* **139**, 31-41.

de Pater, E., Clijsters, L., Marques, S. R., Lin, Y. F., Garavito-Aguilar, Z. V., Yelon, D. and Bakkers, J. (2009). Distinct phases of cardiomyocyte differentiation regulate growth of the zebrafish heart. *Development* **136**, 1633-1641.

Dyer, L. A. and Kirby, M. L. (2009). Sonic hedgehog maintains proliferation in secondary heart field progenitors and is required for normal arterial pole formation. *Dev. Biol.* **330**, 305-317.

Flagg, T. P., Kurata, H. T., Masia, R., Caputa, G., Magnuson, M. A., Lefer, D. J., Coetzee, W. A. and Nichols, C. G. (2008). Differential structure of atrial and ventricular KATP: atrial KATP channels require SUR1. *Circ. Res.* **103**, 1458-1465.

Foglia, M. J., Cao, J., Tornini, V. A. and Poss, K. D. (2016). Multicolor mapping of the cardiomyocyte proliferation dynamics that construct the atrium. *Development* **143**, 1688-1696.

Garavito-Aguilar, Z. V., Riley, H. E. and Yelon, D. (2010). Hand2 ensures an appropriate environment for cardiac fusion by limiting Fibronectin function. *Development* **137**, 3215-3220.

Garcia-Martinez, V. and Schoenwolf, G. C. (1993). Primitive-streak origin of the cardiovascular system in avian embryos. *Dev. Biol.* **159**, 706-719.

George, V., Colombo, S. and Targoff, K. L. (2015). An early requirement for nkx2.5 ensures the first and second heart field ventricular identity and cardiac function into adulthood. *Dev. Biol.* **400**, 10-22.

Hami, D., Grimes, A. C., Tsai, H.-J. and Kirby, M. L. (2011). Zebrafish cardiac development requires a conserved secondary heart field. *Development* **138**, 2389-2398.

Huang, C.-J., Tu, C.-T., Hsiao, C.-D., Hsieh, F.-J. and Tsai, H.-J. (2003). Germ-line transmission of a myocardium-specific GFP transgene reveals critical regulatory elements in the cardiac myosin light chain 2 promoter of zebrafish. *Dev. Dynam.* **228**, 30-40.

Ilagan, R., Abu-Issa, R., Brown, D., Yang, Y.-P., Jiao, K., Schwartz, R. J., Klingensmith, J. and Meyers, E. N. (2006). Fgf8 is required for anterior heart field development. *Development* **133**, 2435-2445.

Keegan, B. R., Meyer, D. and Yelon, D. (2004). Organization of cardiac chamber progenitors in the zebrafish blastula. *Development* **131**, 3081-3091.

Kelly, R. G. (2012). The second heart field. *Curr. Top. Dev. Biol.* **100**, 33-65.

Keren-Politansky, A., Keren, A. and Bengal, E. (2009). Neural ectoderm-secreted FGF initiates the expression of Nkx2.5 in cardiac progenitors via a p38 MAPK/CREB pathway. *Dev. Biol.* **335**, 374-384.

Koibuchi, N. and Chin, M. T. (2007). CHF1/Hey2 plays a pivotal role in left ventricular maturation through suppression of ectopic atrial gene expression. *Circ. Res.* **100**, 850-855.

Lazic, S. and Scott, I. C. (2011). Mef2cb regulates late myocardial cell addition from a second heart field-like population of progenitors in zebrafish. *Dev. Biol.* **354**, 123-133.

Lee, K.-H., Xu, Q. H. and Breitbart, R. E. (1996). A new tinman-related gene, nkx2.7, anticipates the expression of nkx2.5 and nkx2.3 in zebrafish heart and pharyngeal endoderm. *Dev. Biol.* **180**, 722-731.

Lee, Y., Grill, S., Sanchez, A., Murphy-Ryan, M. and Poss, K. D. (2005). Fgf signaling instructs position-dependent growth rate during zebrafish fin regeneration. *Development* **132**, 5173-5183.

Lepilina, A., Coon, A. N., Kikuchi, K., Holdway, J. E., Roberts, R. W., Burns, C. G. and Poss, K. D. (2006). A dynamic epicardial injury response supports progenitor cell activity during zebrafish heart regeneration. *Cell* **127**, 607-619.

Marques, S. R., Lee, Y., Poss, K. D. and Yelon, D. (2008). Reiterative roles for FGF signaling in the establishment of size and proportion of the zebrafish heart. *Dev. Biol.* **321**, 397-406.

McGrath, M. F. and de Bold, A. J. (2009). Transcriptional analysis of the mammalian heart with special reference to its endocrine function. *BMC Genomics* **10**, 254.

Mohammadi, M., McMahon, G., Sun, L., Tang, C., Hirth, P., Yeh, B. K., Hubbard, S. R. and Schlessinger, J. (1997). Structures of the tyrosine kinase domain of fibroblast growth factor receptor in complex with inhibitors. *Science* **276**, 955-960.

Park, E. J., Ogden, L. A., Talbot, A., Evans, S., Cai, C.-L., Black, B. L., Frank, D. U. and Moon, A. M. (2006). Required, tissue-specific roles for Fgf8 in outflow tract formation and remodeling. *Development* **133**, 2419-2433.

Redkar, A., Montgomery, M. and Litvin, J. (2001). Fate map of early avian cardiac progenitor cells. *Development* **128**, 2269-2279.

Reifers, F., Böhli, H., Walsh, E. C., Crossley, P. H., Stainier, D. Y. and Brand, M. (1998). Fgf8 is mutated in zebrafish acerebellar (ace) mutants and is required for maintenance of midbrain-hindbrain boundary development and somitogenesis. *Development* **125**, 2381-2395.

Reifers, F., Walsh, E. C., Léger, S., Stainier, D. Y. and Brand, M. (2000). Induction and differentiation of the zebrafish heart requires fibroblast growth factor 8 (fgf8/acerebellar). *Development* **127**, 225-235.

Schoenebeck, J. J., Keegan, B. R. and Yelon, D. (2007). Vessel and blood specification override cardiac potential in anterior mesoderm. *Dev. Cell* **13**, 254-267.

Schumacher, J. A., Bloomekatz, J., Garavito-Aguilar, Z. V. and Yelon, D. (2013). tal1 regulates the formation of intercellular junctions and the maintenance of identity in the endocardium. *Dev. Biol.* **383**, 214-226.

Simões, F. C., Peterkin, T. and Patient, R. (2011). Fgf differentially controls cross-antagonism between cardiac and haemangioblast regulators. *Development* **138**, 3235-3245.

Soroldoni, D., Hogan, B. M. and Oates, A. C. (2009). Simple and efficient transgenesis with meganuclease constructs in zebrafish. *Methods Mol. Bio.* **546**, 117-130.

Sorrell, M. R. J. and Waxman, J. S. (2011). Restraint of Fgf8 signaling by retinoic acid signaling is required for proper heart and forelimb formation. *Dev. Biol.* **358**, 44-55.

Stainier, D. Y., Lee, R. K. and Fishman, M. C. (1993). Cardiovascular development in the zebrafish. I. Myocardial fate map and heart tube formation. *Development* **119**, 31-40.

Targoff, K. L., Colombo, S., George, V., Schell, T., Kim, S.-H., Solnica-Krezel, L. and Yelon, D. (2013). Nkx genes are essential for maintenance of ventricular identity. *Development* **140**, 4203-4213.

Thomas, N. A., Koudijs, M., van Eeden, F. J., Joyner, A. L. and Yelon, D. (2008). Hedgehog signaling plays a cell-autonomous role in maximizing cardiac developmental potential. *Development* **135**, 3789-3799.

Tirosh-Finkel, L., Zeisel, A., Brodt-Ivenshitz, M., Shamai, A., Yao, Z., Seger, R., Domany, E. and Tzahor, E. (2010). BMP-mediated inhibition of FGF signaling promotes cardiomyocyte differentiation of anterior heart field progenitors. *Development* **137**, 2989-3000.

Wu, S.-P., Cheng, C.-M., Lanz, R. B., Wang, T., Respress, J. L., Ather, S., Chen, W., Tsai, S.-J., Wehrens, X. H. T., Tsai, M.-J. et al. (2013). Atrial identity is determined by a COUP-TFII regulatory network. *Dev. Cell* **25**, 417-426.

Xin, M., Small, E. M., van Rooij, E., Qi, X., Richardson, J. A., Srivastava, D., Nakagawa, O. and Olson, E. N. (2007). Essential roles of the bHLH transcription factor Hrt2 in repression of atrial gene expression and maintenance of postnatal cardiac function. *Proc. Natl. Acad. Sci. USA* **104**, 7975-7980.

Yelon, D., Horne, S. A. and Stainier, D. Y. R. (1999). Restricted expression of cardiac myosin genes reveals regulated aspects of heart tube assembly in zebrafish. *Dev. Biol.* **214**, 23-37.

Yutzey, K. E., Rhee, J. T. and Bader, D. (1994). Expression of the atrial-specific myosin heavy chain AMHC1 and the establishment of anteroposterior polarity in the developing chicken heart. *Development* **120**, 871-883.

Zeng, X.-X. I. and Yelon, D. (2014). Cadm4 restricts the production of cardiac outflow tract progenitor cells. *Cell Rep.* **7**, 951-960.

Zhang, R. L., Han, P. D., Yang, H. B., Ouyang, K. F., Lee, D., Lin, Y.-F., Ocorr, K., Kang, G. S., Chen, J., Stainier, D. Y. R. et al. (2013). In vivo cardiac reprogramming contributes to zebrafish heart regeneration. *Nature* **498**, 497-501.

Zhou, Y., Cashman, T. J., Nevis, K. R., Obregon, P., Carney, S. A., Liu, Y., Gu, A., Mosimann, C., Sondalle, S., Peterson, R. E. et al. (2011). Latent TGF-beta binding protein 3 identifies a second heart field in zebrafish. *Nature* **474**, 645-648.